Atmospheric Pollution Research 10 (2019) 455–461

HOSTED BY

Contents lists available at ScienceDirect

Atmospheric Pollution Research

journal homepage: www.elsevier.com/locate/apr

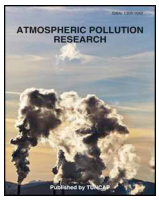

Arsenic accumulation and speciation in epilithic moss collected from an abandoned mercury mining area, south-western China

Longchao Liang[a], Zhidong Xu[b], Guangle Qiu[b], Pan Wu[a,c,*], Ruixue Zhang[a]

[a] Guizhou University, Guiyang 550025, China
[b] State Key Laboratory of Environmental Geochemistry, Institute of Geochemistry, Chinese Academy of Sciences, Guiyang 550081, China
[c] Key Laboratory of Karst Environment and Geohazard, Ministry of Land and Resources, Guiyang 550025, China

ARTICLE INFO

Keywords:
Epilithic moss
Arsenic
Arsenic speciation
Characteristics and spatial distribution
Potential sources

ABSTRACT

Arsenic (As) is considered a carcinogenic toxin, and nonferrous metal smelting activities can release significant quantities of As, causing an increase in As levels in the environment. A total of 221 samples of moss belonging to 5 species in 4 families were collected from the Wanshan District, the world third largest mercury mining area, in Guizhou Province, southwestern China, for analysis of total As (tAs) concentrations and As speciation. The results indicated that the tAs concentrations in these mosses ranged from 0.67 to 9.6 mg kg^{-1}, with an average of 2.4 ± 1.7 mg kg^{-1}. The dominant species of As in these mosses were inorganic forms of arsenite (As(III)) and arsenate (As(V)) with a total percentage of 87%, whereas the concentrations of organic forms (monomethylarsonic acid (MMA) and dimethylarsinic acid (DMA)) were relatively low, with percentages of 11.8% and 6.0%, respectively. A significant correlation ($r = 0.766$, $p < 0.01$) was observed between As(V) and tAs. In the spatial distribution pattern of As, high concentrations of As in mosses were centralized around historical Hg retorting sites in the town of Wanshan, the villages of Gouxi and Yanwuping and sites downwind of these locations, suggesting that historical intensive Hg mining activities might be the most possible source of atmospheric As.

1. Introduction

Toxic arsenic (As) and its chemical compounds are considered some of the most dangerous carcinogens. As is ubiquitous in the natural environment and can enter the human body through skin absorption, respiration, and oral intake (Liu et al., 2007). Long-term As exposure may increase the risks of diabetes, cardiovascular disease, nerve dysfunction, and prostate cancer (Cantor and Lubin, 2007; Coronado-Gonzalez et al., 2007; Boamponsem et al., 2010). Arsenic poisoning cases have been reported around the world (IARC, 2004). In China, for instance, notorious chronic arsenicosis occurred in thousands of inhabitants in the Hetao Basin of Inner Mongolia Province due to their drinking of As-contaminated groundwater (Guo et al., 2003). Recently, in West Bengal, arsenicosis caused by dietary exposure was reported (Golui et al., 2017).

Both anthropogenic and natural sources can release As into the environment. The main natural sources are volcanic activity, weathering, and biological activities (Wedepohl, 1991; Chen et al., 2012). Volcanic activity can release amounts of fine particle-bound As, which remains in atmospheric aerosols and undergoes long-range transport (Wang et al., 2010; Chen et al., 2012; Fang et al., 2012). The anthropogenic sources consist of nonferrous metal smelting, fossil fuel combustion, traffic, fertilizers, and pesticides (Qi et al., 2016; Jandacka et al., 2017; Leclerc and Laurent, 2017; Novillo et al., 2017). Coal-fired energy production and traffic emissions are generally considered the major sources of atmospheric As in urban areas (Pacyna and Pacyna, 2002). Due to increasing industrialization, the As levels in soil, water, air, and biota have increased sharply within the last few decades (Chai et al., 2015; Boente et al., 2017; Sawidis et al., 2012).

Arsenic exists in both organic and inorganic forms in the environment. Organic As includes arsenocholine (AsC), arsenobetaine (AsB), arsenosugars (AsS), monomethylarsonic acid (MMA), and dimethylarsinic acid (DMA), and inorganic As includes arsenate (As(V)) and arsenite (As(III)). The latter exists in the environment highly depends on pH and redox conditions (Ansari and Sadegh, 2007; Zaccone et al., 2018). Different chemical forms of As exhibit different toxicity. Generally, the inorganic As(iAs) forms As(III) and As(V) are more toxic than organic As (oAs) (Styblo et al., 2000; Mass et al., 2001; Geng et al.,

Peer review under responsibility of Turkish National Committee for Air Pollution Research and Control.
* Corresponding author. Guizhou University, Guiyang 550025 China.
E-mail address: pwu@gzu.edu.cn (P. Wu).

https://doi.org/10.1016/j.apr.2018.09.005
Received 6 May 2018; Received in revised form 4 September 2018; Accepted 4 September 2018
Available online 07 September 2018

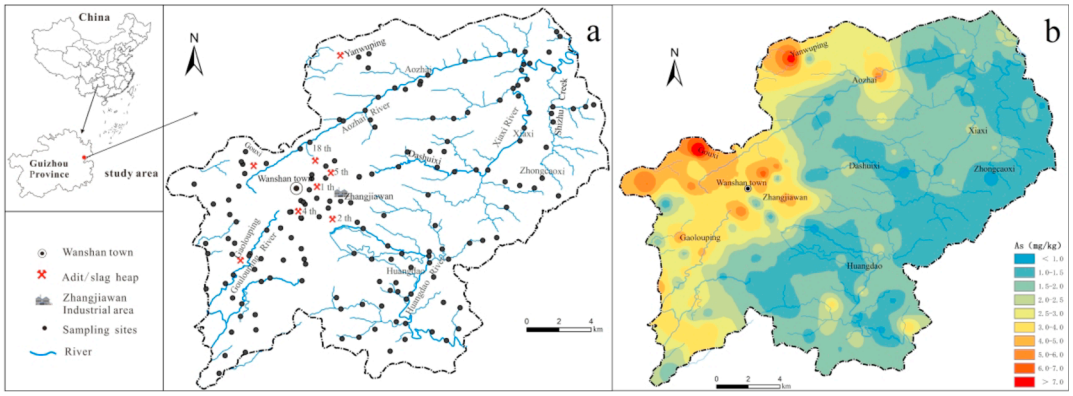

Fig. 1. Map of sampling sites and spatial distributions of total concentrations of As in mosses in the study area.

2009). In contrast, AsB and AsS are nontoxic forms (Francesconi et al., 2002; Raml et al., 2005). In neutral solution, As(III), As(V), MMA, and DMA can occur as anionic species, AsC as a cationic species, and AsB as a zwitterionic species (Zmozinski et al., 2015).

Mosses are primitive terrestrial higher plants and are characterized by a simple structure and large surface area as well as no real root systems, taking up nutrients mainly from the atmosphere (Pott and Turpin, 1996; Aceto et al., 2003; Szczepaniak and Biziuk, 2003; Villares et al., 2016). Due to their special morphological and physiological characteristics, mosses exhibit a certain ability for ion exchange and can capture particulate matter from the atmosphere (Perez-Llamazares et al., 2011; Spagnuolo et al., 2011); therefore, these plants are used for the monitoring of atmospheric pollution (e.g., Galsomiès et al., 1999; Ermakova et al., 2004; Donovan et al., 2016; Shotyk et al., 2015). Currently, utilizing moss to elucidate atmospheric pollutants has become a major global research hotspot (Allajbeu et al., 2016; Zinicovscaia et al., 2017; Wu et al., 2016; Galhardi et al., 2017). Many mosses have been used for monitoring atmospheric nitrogen deposition and heavy metal pollution, such as *Sphagnum girgensohnii* (Vuković et al., 2015), *Isothecium stoloniferum* (Pott and Turpin, 1996), *Pleurozium schreberi* (Goltsova and Vasina, 1995), *Polytrichum juniperinum* (Wolterbeek et al., 1995), and *Haplocladium microphyllum* (Dong et al., 2017), and *Sphagnum* moss (Shotyk et al., 2015). Shotyk et al. (2015, 2016) reported that species of *Sphagnum* could well retain the atmospheric Pb from high temperature combustion and found that the concentrations of Pb in *Sphagnum* were far below the values reported within the past decades thanks to the anthropogenic emissions controlling. Recently, Kempter et al. (2017a, b) reported that modeled data showed the living *Sphagnum* is a good indicator of atmospheric deposition, at least in a semi-quantitative manner and certainly reflects inputs to terrestrial ecosystems.

The Wanshan District is located in Guizhou Province, southwestern China, and once was the third largest mercury (Hg) mining region in the world. The history of Hg mining dates back to 221 B.C. (Qiu et al., 2005) and has caused heavy Hg contamination in the environment (Horvat et al., 2003; Qiu et al., 2005, 2008; 2012, 2013; Dai et al., 2013). Because the dominant cinnabar ores are commonly associated with As present in a wide concentration range of 0.5–28 mg kg^{-1} (Hua and Cui, 1995), contamination by As has also occurred in the environment due to its release from the retorting process of cinnabar ores (Garcia-Ordiales et al., 2018).

To date, no study on the As concentrations and speciation in mosses has been conducted to reveal the atmospheric As pollution in the environment impacted by historic intensive Hg retorting activities in the Wanshan region. The main goal of the present study was to: (1) characterize the total As concentrations and their spatial distribution in mosses; (2) explore speciation of As and their correlations; (3) elucidate atmospheric As pollution and its potential source in abandoned Hg mining areas.

2. Materials and methods

2.1. Study area

The Wanshan District (E: 109º07′-109º24′; N: 27º24′-27º38′) is located in eastern Guizhou Province, southwestern China, and covers an area of 45 km^2. This district is hilly and karstic and has a subtropical humid climate characterized by abundant yearly precipitation of 1200–1400 mm and an annual temperature of 15 °C on average. The major rivers that run through the study area include the Gaolouping, Aozhai, Huangdao, and Xiaxi (Fig. 1a). All of these rivers belong to Yuanjiang tributary and afflux into Dongting Lake in Hunan Province.

The Wanshan District, the largest Hg production center in China, is enriched in cinnabar ore resources. The Hg mining activities ceased in 2001 (Qiu et al., 2005). The dominant ore in the Wanshan Hg mine is cinnabar. Metacinnabar, selenide Hg compounds and elemental Hg also occur there. Generally, the cinnabar ore is associated with pyrite, sphalerite, realgar, and orpiment (Hua and Cui, 1995). The realgar and orpiment are mainly distributed along the edges of deposits. Throughout the mining and retorting history, approximately 20×10^3 tons of Hg have been produced (Zhang et al., 2004). In the process of cinnabar ore smelting, both Hg and As are released into the environment (Garcia-Ordiales et al., 2018).

2.2. Sample collection and preparation

A total of 221 epilithic moss samples were collected from 181 sites in the Wanshan District in September 2014, of which 144 sites were for one species (a total of 144), 34 sites for two species (a total of 68), and 3 sites for three species (a total of 9) (Fig. 1). At each sampling site, a final sample was composed of 3–5 subsamples from several localities within an area of 100 m^2. All sampled mosses were naturally growing on surface of rocks that located in open sites at the least of 500 m away from trees and dwarf shrubs, being sure that all mosses directly exposed to atmospheric deposition (Shotyk et al., 2015). To guarantee the moss have same age, only green and healthy parts (top 2–3 cm) of mosses were collected according to the methodology applied by Xiao et al. (2011), Kempter et al. (2017a), Shotyk et al. (2015). The samples were stored in polyethylene bags to avoid cross-contamination. After collection, samples were delivered to the laboratory, thoroughly washed with Milli-Q water (DW), air-dried and ground with a grinding machine (IKA-A11, Germany).

Species of mosses were identified according to the atlas “Moss Flora of China,” and the microstructures of mosses were observed with an anatomical lens (HWG-1) and a microscope (XSZ-107) (Wu, 2011; Liu et al., 2018). Samples were classified into 5 species in 4 families. Among all the mosses in the present study, *Hypnum plumaeforme* species were the most widely distributed throughout the study area, followed by *Thuidium kanedae* and *Brachythecium buchananii*, accounting for 90%

of the total, and approximately 10% of the total was accounted for by *Entodon acutifolius* and *Brachythecium glareosum*.

2.3. Sample analysis

2.3.1. Total As (tAs)

For total As (tAs) analysis, approximately 0.1 g was digested with 2.5 mL of concentrated subboiling ultrapure HNO_3 (Sinopharm, Shanghai) in a Teflon vessel. The Teflon vessel was placed in a steel can and heated in an oven at 160 °C for 24 h. After the vessel had cooled, 1 mL of H_2O_2 was added to the digested solution and vaporized on an electric heating panel. When the solution crystallized, 1 mL of subboiling ultrapure HNO_3 was added, and the solution was recrystallized. Next, 3 mL of subboiling ultrapure HNO_3 and 2 mL of DW were added, and the solution was heated at 150 °C for 10 h. After cooling, the digestate was centrifuged, filtered through a 0.22 μm cellulose acetate membrane (Pall, USA) and diluted with DW to 50 mL for analysis.

Concentrations of tAs were measured using inductively coupled plasma mass spectrometry (ICP-MS) (Agilent 7700, USA). Helium gas was used in the collision cell to reduce interferences with the ICP-MS measurements, and the gas flow rate was 0.34 mL/min. A solution of ^{103}Rh was used as the internal standard.

2.3.2. Species of As

A total of 40 moss samples of all 5 species, *H. plumaeforme* (n = 11), *T. kanedae* (n = 9), *B. buchananii* (n = 9), *E. acutifolius* (n = 7), and *B. glareosum* (n = 4), were selected for As speciation analysis. Species of As(III), As(V), MMA, and DMA were extracted according to the extraction process (Pizarro et al., 2003). In brief, 0.5 g of a moss sample was accurately weighed into a polytetrafluoroethylene (PTFE) vessel containing 20 mL of 1% subboiling ultrapure HNO_3 and extracted in a microwave extractor at 90 °C for 1.5 h. Then, the samples were centrifuged at 9000 rpm for 30 min. After filtration through a 0.22 μm cellulose acetate membrane (Pall, USA), the supernatant was collected and stored at 4 °C for analysis.

Chromatographic separation of As species was performed on a PRP-X100 anion-exchange column (Hamilton, 4.1 × 250 mm, 10 m). The mobile phase consisted of 4 mM ammonium bicarbonate (NH_4HCO_3, ≥99.99%) at pH 8.6 as phase A and 40 mM ammonium nitrate (NH_4NO_3, ≥98.5%) and 4 mM ammonium bicarbonate (NH_4HCO_3, ≥99.99%) at pH 8.6 as phase B. Ammonia solution (NH_3H_2O, ≥99.99%) was adopted to adjust the pH values. All reagents mentioned above were purchased from Aladdin Reagent Co. Ltd., Shanghai, China. Arsenic species were separated by an HPLC system (Agilent 1290, Germany) and quantified by an Agilent 7700 ICP-MS system. The operating parameters for HPLC-ICP-MS were reported by Ma et al. (2016).

2.4. Contamination factor (CF) calculation

The contamination factor (CF) is considered an index for the qualification of a metal's contamination levels. It is defined as the ratio between the concentration of an element (CM) and the background level (CB). The higher the CF is, the greater the contamination level. Fernández and Carballeira (2001) have categorized CF contamination levels into 5 groups: CF ≤ 1, no contamination; 1 < CF ≤ 2, suspected contamination; 2 < CF ≤ 3.5, slight contamination; 3.5 < CF ≤ 8, moderate contamination; 8 < CF ≤ 27, severe contamination, and CF > 27 extreme contamination (Table 1). In the present study, the value of CB referred to the data reported by Carballeira and López (1997) and Carballeira et al. (2002), which was 0.2 mg kg^{-1} in H. cupressiforme in Galicia, NW Spain. The CF of As in the moss was calculated as:

$$CF = \frac{CM}{CB}$$

where

CF is the contamination factor of As
CM is the concentration of As in the samples
CB is the concentration of As in the control samples

2.5. QA/QC

The quality assurance and quality control of the tAs determination were based on blanks, method blanks, duplicates, and certified reference materials (GBW10020, BCR-482). Approximately 25% of the samples were analyzed in duplicate to check the total variation due to the sampling, and the results of duplicates agreed with each other with an average RSD (%) of 7%. The measured values in the reference samples GBW10020 and BCR-482 were in agreement with the certified values, with recoveries ranging between 88% and 101%. The method blank was below the limit of 0.01 μg L^{-1} of the ICP-MS detector.

For individual As species, the extraction efficiency was evaluated by calculating the ratio between the total concentration of As in the extracted species and the tAs concentration directly measured in samples. The quality control standard solutions were analyzed after constructing the calibration curve. The recoveries obtained in this work varied between 69% and 84%, with an average of 76%. The RSD % value was 6% for BCR-484, and the extraction efficiency was 97%, which is consistent with previous studies (Zmozinski et al., 2015).

2.6. Data analysis

The data were statistically analyzed by Excel software (Microsoft Corp). Significant differences were determined by one-way ANOVA using SPSS 20.0 software (IBM, Inc.). The correlations of tAs with the arsenic species concentrations in the moss samples were analyzed by regression analysis with Origin 8.0 (OriginLab). To better interpret the overall tAs distribution in the mosses in the study area, we processed the large data sets available for the overall Wanshan area studied in the present work using ArcGIS 10.2 (ESRI). The contour map was based on the mean values, and the data were transformed into continuous surfaces by a universal Kriging interpolation technique.

Table 1
Total As concentrations in mosses and their percentages of contamination factors (CF).

Species	As concentration		Category contamination			
	Range	Mean	2 < CF ≤ 3.5	3.5 < CF ≤ 8	8 < CF ≤ 27	27 < CF
B. buchananii	0.98–9.6	3.48 ± 2.40	–	–	100	–
B. glareosum	1.7–3.5	2.48 ± 0.79	–	23	56	21
E. acutifolius	1.4–4.7	2.94 ± 0.99	–	7	93	–
H. plumaeforme	0.67–8.9	1.88 ± 1.29	1	54	41	4
T. kanedae	0.67–6.0	2.32 ± 1.19	2	37	59	2

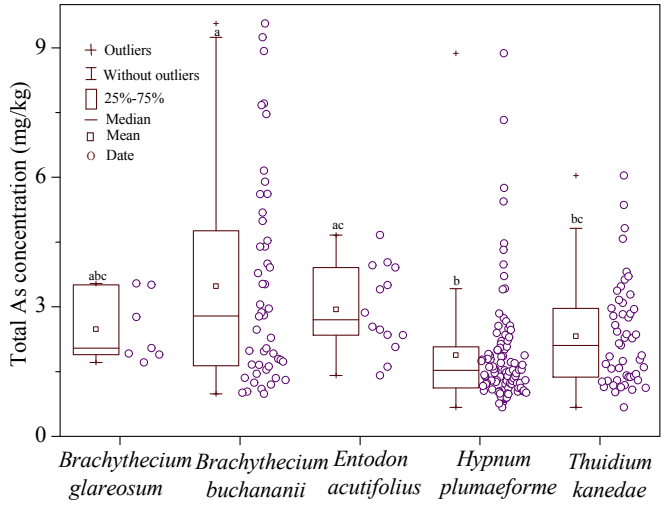

Fig. 2. Total concentrations of As in five species in the study area (Box plot top with the same letter do not differ for $p < 0.05$).

3. Results and discussion

3.1. Total As concentrations

The tAs concentration in mosses (n = 221) ranged widely from 0.67 to 9.6 mg kg^{-1}, with an average of 2.4 ± 1.7 mg kg^{-1}. The species *H. plumaeforme*, the most widely distributed species, exhibited rather low As concentrations, ranging from 0.67 to 8.9 mg kg^{-1}, with an average of 1.9 ± 1.3 mg kg^{-1} (Fig. 2). Among the five moss species, *B. buchananii* exhibited the highest As concentrations, ranging from 0.98 to 9.6 mg kg^{-1}, with an average of 3.5 ± 2.4 mg kg^{-1}, followed by *E. acutifolius* (range: 1.4–4.7 mg kg^{-1}, average: 2.9 ± 0.99 mg kg^{-1}), *B. glareosum* (range: 1.7–3.5 mg kg^{-1}, average: 2.5 ± 0.79 mg kg^{-1}), and *T. kanedae* (range: 0.67–6.0 mg kg^{-1}, average: 2.3 ± 1.2 mg kg^{-1}) (Table 1). Significant differences ($p < 0.05$) were obtained between *H. plumaeforme* and *B. buchananii*, *H. plumaeforme* and *E. acutifolius*, as well as *B. buchananii* and *T. kanedae* (Fig. 2). The differences in the tAs concentrations observed in moss species may suggest their different abilities for As accumulation (Szczepaniak and Biziuk, 2003; Fernández et al., 2002). However, an alternative explanation might be attributing for the variations of atmospheric As concentrations in ambient air caused by Hg smelting activities.

Compared with the results obtained in other areas of the world (Table 2), the concentrations of tAs in mosses from Wanshan were higher than those observed in *H. cupressiforme* from a pyrite mining district reported by Bargagli et al. (2002), which contained 1.4 ± 1.3 mg kg^{-1} on average, but were lower than those found in mosses from abandoned Pyrenees zinc-lead smelting areas in Spain, which reached up to 34 ± 3.0 mg kg^{-1} (Marques et al., 2003), and from lead-zinc smelting areas in Sebinkarahisar in Turkey (17 mg kg^{-1}) (Koz, 2014). In contrast, mosses from nonpolluted areas contained low levels of tAs, with average values ranging from 0.26 to 0.40 mg kg^{-1} (Fernández et al., 2002). In *Sphagnum* from bogs of Athabasca areas in Canada, the As concentration was 0.43 ± 0.26 mg kg^{-1} on average (Shotyk et al., 2016), and from 0.079 to 0.705 mg kg^{-1} in bogs of southern German (Kempter et al., 2017a). The high concentrations of tAs found in mosses from Hg mining and lead-zinc smelting areas verify that nonferrous metals smelting activities are an important anthropogenic source of atmospheric As (Koz, 2014). Furthermore, a significant positive correlation ($r = 0.82$, $p < 0.01$) was observed between tAs and Hg (data was unpublished) in moss samples, reflecting a dominant source of atmospheric As was related to Hg smelting activities.

3.2. Spatial distribution

Fig. 1b shows that the high concentrations of tAs were generally centralized around the town of Wanshan and the villages of Gouxi and Yanwuping. The maximum value was observed at the Gouxi site, and the minimum value was observed at the Zhongcai site. Evidently, this reflects the influence of the surroundings, which, at these locations, were greatly affected by historical intensive Hg mining activities (Qiu et al., 2005). The northwest direction seems to be the primary direction of As dispersion in the Wanshan District. Generally, there existed a decreasing arsenic concentration from northwest to southeast. The low concentrations of As in mosses were detected southeast of the Wanshan District, where Hg mining and retorting facilities are located.

These distribution patterns suggested that historical Hg mining and retorting activities are the dominant source of the As in the moss. During the process of intensive cinnabar ore retorting, As could be released associated with Hg and result in an increase in atmospheric As, which eventually deposits and is absorbed by moss (Perez-Llamazares et al., 2011). Numerous abandoned retorting facilities were located in or near Wanshan town and Yanwuping village. In Gouxi, historical artisanal Hg retorting sites were observed. Those historical Hg retorting activities might explain the elevated concentrations of As in mosses growing within those areas.

In addition, during our study period, several large factories related to Hg chemical compound manufacturing were in operation at the site of Zhangjiawan, which may also have released As into the atmosphere during manufacturing processes that are combined with coal combustion (Coskun et al., 2011; Yan et al., 2016). The fine particle-bound As emitted to the atmosphere under the influence of the dominant wind in the northeast direction could lead to a high deposition of As and increased As levels in mosses in the southwest area of the region (Villares et al., 2016).

Table 2
Comparison of total and speciation As in mosses and peat reported in the other areas worldwide (Unit: mg kg^{-1}).

Species	tAs	As(V)	As(III)	DMA	MMA	Reference
B. buchananii	3.5 ± 2.4	2.8 ± 0.79	0.20 ± 0.05	0.11 ± 0.03	0.09 ± 0.03	This study
B. glareosum	2.5 ± 0.79	1.8 ± 0.61	0.19 ± 0.08	0.07 ± 0.02	0.07 ± 0.04	
E. acutifolius	2.9 ± 0.99	2.1 ± 0.19	0.38 ± 0.11	0.17 ± 0.04	0.16 ± 0.03	
H. plumaeforme	1.9 ± 1.3	2.8 ± 1.1	0.26 ± 0.13	0.14 ± 0.05	0.08 ± 0.03	
T. kanedae	2.3 ± 1.2	2.5 ± 0.82	0.33 ± 0.19	0.20 ± 0.08	0.10 ± 0.04	
H. cupressiforme	1.4 ± 1.3					Bargagli et al. (2002)
Pleurocarpus sp	34 ± 3					Marques et al. (2003)
H. sericeum	17.8					Koz, 2014
H. cupressiforme	0.405 ± 0.53					Fernández et al. (2002)
S. purum	0.27 ± 0.27					
Sphagnum	0.43 ± 0.26					Shotyk et al. (2016)
Sphagnum	0.08–0.71					Kempter et al. (2017a)
Peat	1.4 ± 1.2			0.13 ± 0.06	0.09 ± 0.03	Zaccone et al. (2018)

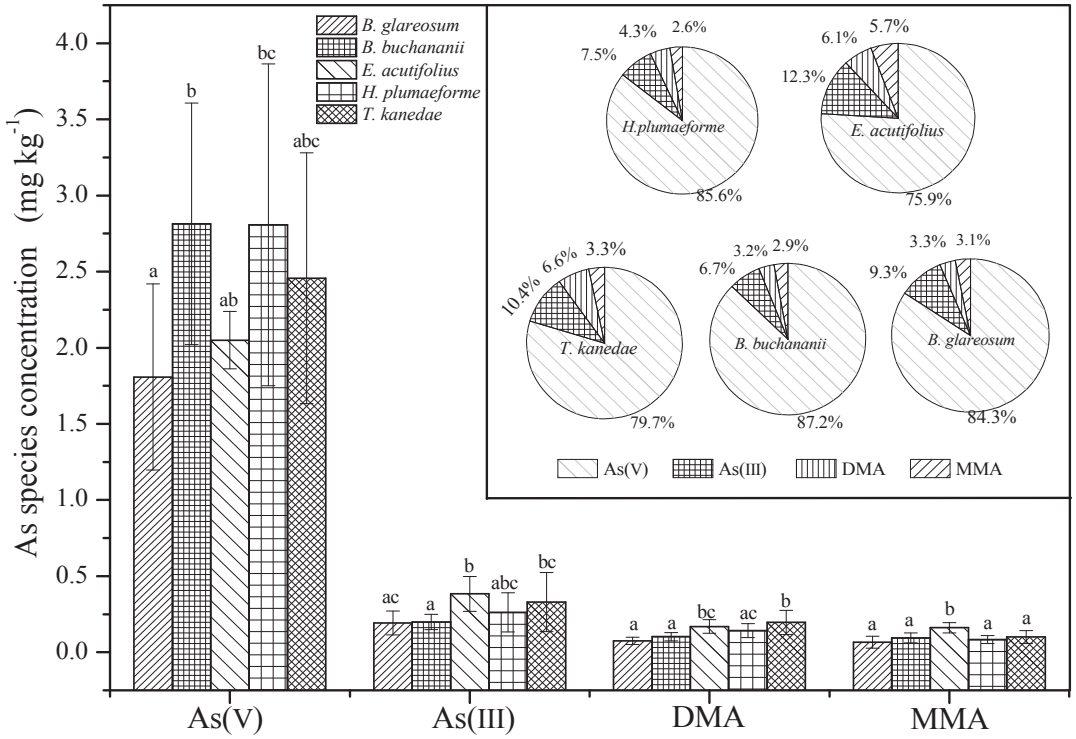

Fig. 3. Species of As and their percentages in mosses (Bar graph top with the same letter do not differ at the 95% confidence level).

3.3. Species of As

Regarding the concentrations of the different arsenic species, As(V) ranged from 0.68 to 6.0 mg kg^{-1} with an average of 2.5 ± 0.85 mg kg^{-1}, As(III) from 0.09 to 0.66 mg kg^{-1} with an average of 0.28 ± 0.14 mg kg^{-1}, DMA from 0.03 to 0.36 mg kg^{-1} with an average of 0.15 ± 0.06 mg kg^{-1}, and MMA from 0.01 to 0.21 mg kg^{-1} with an average of 0.1 ± 0.04 mg kg^{-1}. As(V) was the dominant form, with percentages ranging from 75.9% to 87.2% of the tAs, followed by As(III) with a range of 6.7–12.3%, DMA with a range of 3.2–6.6% and MMA with a range of 2.6–5.7% (Fig. 3). A positive correlation was observed between As(V) and tAs ($r = 0.766$, $p < 0.01$), indicating that the concentration of As(V) in mosses increased significantly with the total arsenic concentration. Moreover, significant positive correlations ($p < 0.01$) were found among As(III), MMA, and DMA (Table 3), reflecting a likely common pathway of arsenite and organic As species transformation. Generally mosses may absorb inorganic As from atmospheric dry and wet deposition, then the process of methylation might occur in their body (Nan et al., 2018; Zaccone et al., 2018); this might be an explanation for the significant correlations among those As species.

Previous studies indicated that the dominant species of As in plants were As(V) and As(III) (Amaral et al., 2013). Additionally, MMA, DMA, AsB, and AsC were reported in rice (Zmozinski et al., 2015). Recently, Zaccone et al. (2018) investigated the methylated arsenic species from a free-floating peat island, and found that organic As species (DMA + MA + TMAO + AB) accounted for 28 ± 10% of tAs (range: 6.0–51%), providing the first evidence of methylated As species. The percentages of inorganic As were high and varied between 88 and 95% in the present study, suggesting that the inorganic As forms play important roles in moss. This may related to the existence forms of As in the environment and inorganic As is the predominant form in water, soil and air (Ansone et al., 2013; Zaccone et al., 2018; Lin et al., 2013). This phenomenon was in accordance with those observed in leafy vegetables and rice samples, except that the concentrations of As(III) were much higher than those of As(V) in these other plants (Ma et al., 2017; Liu et al., 2017), which was attributed to the conversion and transformation of As(V) to As(III) in plants (Ma et al., 2017). In the present study, the high percentages of As(V) in moss might be attributed to the primary pathway of nutrient uptake from the atmosphere by moss (Sloof, 1993), in which the dominant species was As(V), accounting for 79-73% of the atmospheric tAs (Lin et al., 2013; Widziewicz et al., 2016).

Table 3
Correlations among tAs and As species.

	tAs	As (V)	As (III)	DMA	MMA
tAs	1				
As(V)	.766**	1			
As(III)	.023	.186	1		
DMA	.161	.094	.696**	1	
MMA	.039	.098	.572**	.485**	1

**Correlation is significant at the 0.01 level.

3.4. Contamination factors

The results indicated that the CF values ranged from 3.4 to 48, with an average of 12 (Table 1). The CF values of all the samples were greater than 2, suggesting As contamination in the mosses. Extreme contamination levels were found in 21% (n = 2) of *B. buchananii* samples, followed by 4% (n = 4) of *H. plumaeforme* samples and 2% (n = 1) of *T. kanedae* samples. Approximately 41% and 54% of *H. plumaeforme* samples contained in severe and moderate levels, respectively. All As species in *B. glareosum* and 93% of the As species in *E. acutifolius* were detected at severe levels. Usually, in natural habitats, the CF values of aquatic bryophytes are below 6 (Díaz et al., 2013). Recently, Allajbeu et al. (2016) reported an average value of 4.8 for As in moss collected from Albania. Compared with these reported data, our CF results obtained in the Wanshan District are much higher.

4. Conclusions

The total concentrations and speciation of As in samples of epilithic moss (n = 221) belonging to 5 species in 4 families collected from abandoned Hg mining regions were investigated. The results revealed that the mosses in the study area contained highly elevated tAs concentrations, as high as 9.6 mg kg^{-1}, indicating heavy impacts from historical Hg smelting activities. The spatial distribution pattern of the total As in mosses was generally centralized around sites that were greatly affected by historical intensive Hg mining activities, which further confirms that the Hg smelting is the dominant source of As in the moss. Species of As(V) was the dominant form in moss, ranging between 88% and 94.5% of the tAs, and a significant positive correlation ($r = 0.766$, $p < 0.01$) was found between As(V) and tAs. Moreover, significant positive correlations among As(III), MMA, and DMA were observed, reflecting a pathway of transformation among species. Since the moss has a unique structure and taking up nutrients from atmospheric deposition, the abundance of As in moss samples might indicate high levels of atmospheric As in the study area, and high CF values of As obtained in moss also elucidated that the atmosphere in the present study region was heavily impacted by As. A further precise characterization of the toxin accumulation in these epilithic mosses and potential sources of atmospheric As in the study region is required for a better understanding in the future.

Acknowledgements

We sincerely gratitude to reviewers and editors for their critical comments and suggestions on our manuscript, also the help of Dr Xiaohang Xu during the revised of the article. This work was supported by the Chinese National Science Foundation (No. 41463008), Chinese National Science Foundation-Guizhou Provincial People's Government Karst Science Research Center project (U1612442), High Level Talent Training Program in Guizhou ([2016]5664) and The First Class Discipline Construction Project in Guizhou (GNYL[2017]007).

References

Allajbeu, S., Qarri, F., Marku, E., Bekteshi, L., Ibro, V., Frontasyeva, M.V., Stafilov, T., Lazo, P., 2016. Contamination scale of atmospheric deposition for assessing air quality in Albania evaluated from most toxic heavy metal and moss biomonitoring. Air Qual. Atmos. Health 10 (5), 587–599.

Amaral, C.D.B., Nóbrega, J.A., Nogueira, A.R.A., 2013. Sample preparation for arsenic speciation in terrestrial plants-a review. Talanta 115 (22), 291–299.

Ansone, L., Klavins, M., Viksna, A., 2013. Arsenic removal using natural biomaterial-based sorbents. Environ. Geochem. Health 35 (5), 633–642.

Aceto, M., Abollino, O., Conca, R., Malandrino, M., Mentasti, E., Sarzanini, C., 2003. The use of mosses as environmental metal pollution indicators. Chemosphere 50 (3), 333–342.

Ansari, R., Sadegh, M., 2007. Application of activated carbon for removal of arsenic ions from aqueous solutions. J. Chem. 4 (1), 103–108.

Boente, C., Matanzas, N., García-González, N., Rodríguez-Valdés, E., Gallego, J.R., 2017. Trace elements of concern affecting urban agriculture in industrialized areas: a multivariate approach. Chemosphere 183, 546–556.

Boamponsem, L.K., Adam, J.I., Dampare, S.B., Nyarko, B.J.B., Essumang, D.K., 2010. Assessment of atmospheric heavy metal deposition in the Tarkwa gold mining area of Ghana using epiphytic lichens. Nucl. Instrum. Methods Phys. Res., Sect. B 268 (9), 1492–1501.

Bargagli, R., Monaci, F., Borghini, F., Bravi, F., Agnorelli, C., 2002. Mosses and lichens as biomonitors of trace metals. A comparison study on *Hypnum cupressiforme*, and *Parmelia caperata*, in a former mining district in Italy. Environ. Pollut. 116 (2), 279–287.

Chen, B., Stein, A.F., Castell, N., Rosa, J.D.D.L., Campa, A.M.S.D.L., Gonzalez-Castanedo, Y., Draxler, R., 2012. Modeling and surface observations of arsenic dispersion from a large Cu-smelter in southwestern Europe. Atmos. Environ. 49 (7), 114–122.

Cantor, K.P., Lubin, J.H., 2007. Arsenic, internal cancers, and issues in inference from studies of low-level exposures in human populations. Toxicol. Appl. Pharmacol. 222 (3), 252–257.

Coronado-Gonzalez, J.A., Del Razo, L.M., Garcia-Vargas, G., Sanmiguel-Salazar, F., Escobedode, L.P.J., 2007. Inorganic arsenic exposure and type 2 diabetes mellitus in Mexico. Environ. Res. 104 (3), 383–389.

Carballeira, A., Couto, J.A., Fernández, J.A., 2002. Estimation of background levels of various elements in Terrestrial mosses from Galicia (NW Spain). Water, Air, Soil Pollut. 133 (1–4), 235–252.

Chai, Y., Guo, J., Chai, S.L., Cai, J., Xue, L.F., Zhang, Q.W., 2015. Source identification of eight heavy metals in grassland soils by multivariate analysis from the Baicheng-Songyuan area, Jilin Province, Northeast China. Chemosphere 134, 67–75.

Coskun, M., Cayir, A., Coskun, M., Kilic, O., 2011. Heavy metal deposition in moss samples from east and South Marmara region, Turkey. Environ. Monit. Assess. 174 (1–4), 219–227.

Carballeira, A., López, J., 1997. Physiological and statistical methods to identify background levels of metals in aquatic bryophytes: dependence on lithology. J. Environ. Qual. 26 (4), 980–988.

Dai, Z.H., Feng, X.B., Zhang, C., Wang, J.F., Jiang, T.M., Xiao, H.J., Li, Y., Wang, X., Qiu, G.L., 2013. Assessing anthropogenic sources of mercury in soil in Wanshan Hg mining area, Guizhou, China. Environ. Sci. Pollut. Res. 20 (11), 7560–7569.

Díaz, S., Villares, R., López, J., Carballeira, A., 2013. Arsenic and mercury in native aquatic bryophytes: differences among species. Bull. Environ. Contam. Toxicol. 90 (4), 465–470.

Donovan, G.H., Jovan, S.E., Gatziolis, D., Burstyn, I., Michael, Y.L., Amacher, M.C., Monleon, V.J., 2016. Using an epiphytic moss to identify previously unknown sources of atmospheric cadmium pollution. Sci. Total Environ. 559, 84–93.

Dong, Y.P., Liu, X.Y., Sun, X.C., Song, W., Zheng, X.D., Li, R., Liu, C.Q., 2017. Inter-species and intra-annual variations of moss nitrogen utilization: implications for nitrogen deposition assessment. Environ. Pollut. 230 (1), 506–515.

Ermakova, E.V., Frontasyeva, M.V., Steinnes, E., 2004. Air pollution studies in Central Russia (Tula Region) using the moss biomonitoring technique, INAA and AAS. J. Radioanal. Nucl. Chem. 259 (1), 51–58.

Fernández, J.A., Carballeira, A., 2001. A comparison of indigenous mosses and topsoils for use in monitoring atmospheric heavy metal deposition in Galicia (northwest Spain). Environ. Pollut. 114 (3), 431–441.

Fernández, J.A., Ederra, A., Núñez, E., Martínez-Abaigar, J., Infante, M., Heras, P., Elías, M.J., Maximpaka, V., Carballeira, A., 2002. Biomonitoring of metal deposition in northern Spain by moss analysis. Sci. Total Environ. 300 (1–3), 115–127.

Fang, G.C., Huang, J.H., Liu, C.K., Huang, Y.L., 2012. Measuring and modeling atmospheric arsenic pollutants, total As, As(III), and As(V), at five characteristic sampling sites. Aerosol Air Qual Res. 12 (2), 200–210.

Francesconi, K.A., Tanggaar, R., Mckenzie, C.J., Goessler, W., 2002. Arsenic metabolites in human urine after ingestion of an arsenosugar. Clin. Chem. 48 (1), 92–101.

Guo, X.J., Fujino, Y., Chai, J.S., Wu, K.G., Xia, Y.J., Li, Y.H., Lv, J.G., Sun, Z.M., Yoshimura, T., 2003. The prevalence of subjective symptoms after exposure to arsenic in drinking water in Inner Mongolia, China. J. Epidemiol. 13 (4), 211–215.

Geng, W.H., Komine, R., Ohta, T., Nakajima, T., Takanashi, H., Ohki, A., 2009. Arsenic speciation in marine product samples: comparison of extraction-HPLC method and digestion-cryogenic trap method. Talanta 79 (2), 369–375.

Golui, D., Guha Mazumder, D.N., Sanyal, S.K., Datta, S.P., Ray, P., Patra, P.K., Sarkar, S., Bhattacharya, K., 2017. Safe limit of arsenic in soil in relation to dietary exposure of arsenicosis patients from Malda district, West Bengal-A case study. Ecotoxicol. Environ. Saf. 144, 227–235.

Galsomiès, L., Letrouit, M.A., Deschamps, C., Savanne, D., Avnaim, M., 1999. Atmospheric metal deposition in France: initial results on moss calibration from the 1996 biomonitoring. Sci. Total Environ. 232 (1–2), 39–47.

Galhardi, J.A., García-Tenorio, R., Francés, I.D., Bonotto, D.M., Marcelli, M.P., 2017. Natural radionuclides in lichens, mosses and ferns in a thermal power plant and in an adjacent coal mine area in southern Brazil. J. Environ. Radioact. 167, 43–53.

Garcia-Ordiales, E., Covelli, S., Rico, J.M., Roqueñí, N., Fontolan, G., Flor-Blanco, G., Cienfuegos, P., Loredo, J., 2018. Occurrence and speciation of arsenic and mercury in estuarine sediments affected by mining activities (Asturias, northern Spain). Chemosphere 198, 281–289.

Goltsova, N.I., Vasina, T.V., 1995. The use of bioindication for estimation of pollution in forest ecosystems of the Leningrad region. In: Ecovision World Monograph Series, pp. 141–154.

Hua, Y.F., Cui, M.Z., 1995. Wanshan Mercury Deposit in Guizhou Province. Geological publishing house, Beijing (in Chinese).

Horvat, M., Nolde, N., Fajon, V., Jereb, V., Logar, M., Lojen, S., Jacimovic, R., Falnoga, I., Liya, Q., Faganeli, J., Drobne, D., 2003. Total mercury, methylmercury and selenium in mercury polluted areas in the province Guizhou, China. Sci. Total Environ. 304 (3), 231–256.

International Agency for Research on Cancer (IARC), 2004. Some drinking-water disinfectants and contaminants, including arsenic. IARC Monogr. Eval. Carcinog. Risks Hum. 84, 1–477.

Jandacka, D., Durcanska, D., Bujdos, M., 2017. The contribution of road traffic to particulate matter and metals in air pollution in the vicinity of an urban road. Transp. Res. D-Transp. Environ. 50, 397–408.

Kempter, H., Krachler, M., Shotyk, W., Zaccone, C., 2017a. Major and trace elements in sphagnum, moss from four southern German bogs, and comparison with available moss monitoring data. Ecol. Indicat. 78, 19–25.

Kempter, H., Krachler, M., Shotyk, W., Zaccone, C., 2017b. Validating modelled data on major and trace element deposition in southern Germany using sphagnum, moss. Atmos. Environ. 167, 656–664.

Koz, B., 2014. Energy-dispersive X-ray fluorescence analysis of moss and soil from abandoned mining of Pb-Zn ores. Environ. Monit. Assess. 186 (9), 5315–5326.

Leclerc, A., Laurent, A., 2017. Framework for estimating toxic releases from the application of manure on agricultural soil: National release inventories for heavy metals in 2000-2014. Sci. Total Environ. 590–591, 452–460.

Liu, T., Guo, H.M., Xiu, W., Wei, C., Li, X.M., Di, Z., Song, W., 2017. Biomarkers of arsenic exposure in arsenic-affected areas of the Hetao Basin, Inner Mongolia. Sci. Total Environ. 609, 524–534.

Liu, G.J., Zheng, L.G., Duzgoren-Aydin, N.S., Gao, L.F., Liu, J.H., Peng, Z.C., 2007. Health effects of arsenic, fluorine, and selenium from indoor burning of Chinese coal. Rev.

Environ. Contam. Toxicol. 189, 89–106.
Liu, R., Zhang, Z.H., Shen, J.C., Wang, Z.H., 2018. Analysis of metal content and vertical stratification of epiphytic mosses along a Karst Mountain highway. Environ. Sci. Pollut. Res. 25 (23), 1–9.
Lin, L.F., Wu, S.H., Lin, S.L., Mwangi, J.K., Lin, Y.M., Lin, C.W., Wang, L.C., Chang-Chien, G.P., 2013. Atmospheric arsenic deposition in Chiayi county in southern taiwan. Aerosol Air Qual Res. 13 (3), 932–942.
Marques, A.F., Queralt, I., Carvalho, M.L., Bordalo, M., 2003. Total reflection X-ray fluorescence and energy-dispersive X-ray fluorescence analysis of runoff water and vegetation from abandoned mining of Pb-Zn ores. Spectrochim. Acta, Part B 58 (12), 2191–2198.
Mass, M.J., Tennant, A., Roop, B.C., Cullen, W.R., Styblo, M., Thomas, D.J., Kligerman, A.D., 2001. Methylated trivalent arsenic species are genotoxic. Chem. Res. Toxicol. 14 (4), 355–361.
Ma, L., Wang, L., Tang, J., Yang, Z.G., 2016. Optimization of arsenic extraction in rice samples by Plackett-Burman design and response surface methodology. Food Chem. 204, 283–288.
Ma, L., Wang, L., Tang, J., Yang, Z., 2017. Arsenic speciation and heavy metal distribution in polished rice grown in Guangdong province, Southern China. Food Chem. 233, 110–116.
Nan, K., He, M., Chen, B., Chen, Y., Hu, B., 2018. Arsenic speciation in tree moss by mass spectrometry based hyphenated techniques. Talanta 183, 48–54.
Novillo, O., Pertusa, J.F., Tomás, J., 2017. Exploring the presence of pollutants at sea: monitoring heavy metals and pesticides in loggerhead turtles (*Caretta caretta*) from the western Mediterranean. Sci. Total Environ. 598, 1130–1139.
Pacyna, E.G., Pacyna, J.M., 2002. Global emission of mercury from anthropogenic sources in 1995. Water, Air, Soil Pollut. 137 (1), 149–165.
Perez-Llamazares, A., Fernandez, J.A., Aboal, J.R., Giordano, S., Carballeira, A., 2011. Evaluation of the efficacy of the sequential elution technique, by use of electron microscopy methods. J. Bryol. 33 (1), 54–61.
Pizarro, I., Gómez, M., Cámara, C., Palacios, M.A., 2003. Arsenic speciation in environmental and biological samples: extraction and stability studies. Anal. Chim. Acta 495 (1), 85–98.
Pott, U., Turpin, D.H., 1996. Changes in atmospheric trace element deposition in the Fraser Valley, B.C., Canada from 1960 to 1993 measured by moss monitoring with *Isothecium stoloniferum*. Can. J. Bot. 74 (8), 1345–1353.
Qiu, G.L., Feng, X.B., Wang, S.F., Shang, L.H., 2005. Mercury and methylmercury in riparian soil, sediments, mine-waste calcines, and moss from abandoned hg mines in east Guizhou province, southwestern China. Appl. Geochem. 20 (3), 627–638.
Qiu, G.L., Feng, X.B., Li, P., Wang, S.F., Li, G.H., Shang, L.H., 2008. Methylmercury accumulation in rice (*Oryza sativa L*) grown at abandoned mercury mines in Guizhou, China. J. Agric. Food Chem. 56 (7), 2465–2468.
Qiu, G.L., Feng, X.B., Jiang, G.B., 2012. Synthesis of current data for Hg in areas of geologic resource extraction contamination and aquatic systems in China. Sci. Total Environ. 421–422 (1), 59–72.
Qiu, G.L., Feng, X.B., Meng, B., Zhang, C., Gu, C.H., Du, B.Y., Lin, Y., 2013. Environmental geochemistry of an abandoned mercury mine in Yanwuping, Guizhou province, China. Environ. Res. 125, 124–130.
Qi, J.Y., Zhang, H.L., Li, X.P., Lu, J., Zhang, G.S., 2016. Concentrations, spatial distribution, and risk assessment of soil heavy metals in a Zn-Pb mine district in southern China. Environ. Monit. Assess. 188 (7), 1–11.
Raml, R., Goessler, W., Traar, P., Ochi, T., Francesconi, K.A., 2005. Novel thioarsenic metabolites in human urine after ingestion of an arsenosugar, 2',3'-dihydroxypropyl 5-deoxy-5-dimethylarsinoyl-beta-D-riboside. Chem. Res. Toxicol. 18 (9), 1444–1450.
Shotyk, W., Kempter, H., Krachler, M., Zaccone, C., 2015. Stable (^{206}Pb, ^{207}Pb, ^{208}Pb) and radioactive (^{210}Pb) lead isotopes in 1 year of growth of *Sphagnum* moss from four ombrotrophic bogs in southern Germany: geochemical significance and environmental implications. Geochem. Cosmochim. Acta 163, 101–125.
Shotyk, W., Bicalho, B., Cuss, C.W., Duke, M.J., Noernberg, T., Pelletier, R., Steinnes, E., Zaccone, C., 2016. Dust is the dominant source of "heavy metals" to peat moss (Sphagnum fuscum) in the bogs of the Athabasca Bituminous Sands region of northern Alberta. Environ. Int. 92–93, 494–506.
Sloof, J.E., 1993. Environmental Lichenology: Biomonitoring Trace-element Air Pollution. Ph.D. Thesis. Delft University of Technology, The Netherlands.
Styblo, M., Del Razo, L.M., Vega, L., Germolec, D.R., LeCluyse, E.L., Hamilton, G.A., Reed, W., Wang, C., Cullen, W.R., Thomas, D.J., 2000. Comparative toxicity of trivalent and pentavalent inorganic and methylated arsenicals in rat and human cells. Arch. Toxicol. 74 (6), 289–299.
Spagnuolo, V., Zampella, M., Giordano, S., Adamo, P., 2011. Cytological stress and element uptake in moss and lichen exposed in bags in urban area. Ecotoxicol. Environ. Saf. 74 (5), 1434–1443.
Sawidis, T.L., Krystallidis, P., Veros, D., Chettri, M., 2012. A study of air pollution with heavy metals in Athens city and Attica basin using evergreen trees as biological indicators. Biol. Trace Elem. Res. 148 (3), 396–408.
Szczepaniak, K., Biziuk, M., 2003. Aspects of the biomonitoring studies using mosses and lichens as indicators of metal pollution. Environ. Res. 93 (3), 221–230.
Villares, R., Díaz, S., López, J., Vázquez, M.D., Carballeira, A., 2016. Contribution of atmospheric deposition to tissue concentrations of mercury in aquatic bryophytes. Sci. Total Environ. 565, 249–257.
Vuković, G., Urošević, M.A., Tomašević, M., Samson, R., Popović, A., 2015. Biomagnetic monitoring of urban air pollution using moss bags (*Sphagnum girgensohnii*). Ecol. Indicat. 52, 40–47.
Wolterbeek, H.T., Kuik, P., Verburg, T.G., Herpin, U., Markert, B., Thöni, L., 1995. Moss interspecies comparisons in trace element concentrations. Environ. Monit. Assess. 35 (3), 263–286.
Wu, L.Q., Taylor, M.P., Handley, H.K., Gulson, B.L., 2016. Insights into past atmospheric lead emissions using lead concentrations and isotopic compositions in historic lichens and fungi (1852-2008) from central and southern Victoria, Australia. Atmos. Environ. 139, 46–55.
Wedepohl, K.H., 1991. Chemical composition and fractionation of the continental-crust. Geol. Rundsch. 80 (2), 207–223.
Wang, Y.F., Chao, H.R., Wang, L.C., Chang-Chien, G.P., Tsou, T.C., 2010. Characteristics of heavy metals emitted from a heavy oil-fueled power plant in northern Taiwan. Aerosol Air Qual Res. 10 (2), 111–118.
Widziewicz, K., Rogula-Kozłowska, W., Loska, K., 2016. Cancer risk from arsenic and chromium species bound to $PM_{2.5}$, and PM_1-Polish case study. Atmos. Pollut. Res. 7 (5), 884–894.
Wu, P.C., 2011. In: Moss flora of China, vol. 8 Science Press, Beijing (in Chinese).
Xiao, H.Y., Xie, Z.Y., Tang, C.G., Wang, Y.L., Liu, C.Q., 2011. Epilithic moss as a biomonitor of atmospheric N deposition in South China. J. Geophys. Res. 116, D24301.
Yan, Y., Zhang, Q., Wang, G.G., Fang, Y.M., 2016. Atmospheric deposition of heavy metals in Wuxi, China: estimation based on native moss analysis. Environ. Monit. Assess. 188 (6), 360–368.
Zaccone, C., Lobianco, D., Raber, G., D'Orazio, V., Shotyk, W., Miano, T.M., Francesconi, K., 2018. Methylated arsenic species throughout a 4-m deep core from a free-floating peat island. Sci. Total Environ. 621, 67–74.
Zmozinski, A.V., Llorente-Mirandes, T., López-Sánchez, J.F., Silva, M.M.D., 2015. Establishment of a method for determination of arsenic species in seafood by LC-ICP-MS. Food Chem. 173, 1073–1082.
Zhang, G.P., Liu, C.Q., Wu, P., Yang, Y.G., 2004. The geochemical characteristics of mine-waste calcines and runoff from the Wanshan mercury mine, Guizhou, China. Appl. Geochem. 19 (11), 1735–1744.
Zinicovscaia, I., Hramco, C., Duliu, O.G., Vergel, K., Culicov, O.A., Frontasyeva, M.V., 2017. Air pollution study in the Republic of Moldova using moss biomonitoring technique. Bull. Environ. Contam. Toxicol. 98 (2), 262–269.